Minimal cobalt metabolism in the marine cyanobacterium *Prochlorococcus*

Nicholas J. Hawco[a,b,1,2], Matthew M. McIlvin[a], Randelle M. Bundy[a,c], Alessandro Tagliabue[d], Tyler J. Goepfert[a,e], Dawn M. Moran[a], Luis Valentin-Alvarado[a,f], Giacomo R. DiTullio[g], and Mak A. Saito[a,2]

[a]Department of Marine Chemistry and Geochemistry, Woods Hole Oceanographic Institution, Woods Hole, MA 02543; [b]Department of Earth Sciences, University of Southern California, Los Angeles, CA 90089; [c]School of Oceanography, University of Washington, Seattle, WA 98105; [d]Department of Earth, Ocean and Ecological Sciences, University of Liverpool, Liverpool L69 G3p, United Kingdom; [e]School of Earth and Space Exploration, Arizona State University, Tempe, AZ 85287; [f]Department of Plant and Microbial Biology, University of California, Berkeley, CA 94720; and [g]Hollings Marine Laboratory, College of Charleston, Charleston, SC 29412

Edited by François M. M. Morel, Princeton University, Princeton, NJ, and approved May 15, 2020 (received for review January 27, 2020)

Despite very low concentrations of cobalt in marine waters, cyanobacteria in the genus *Prochlorococcus* retain the genetic machinery for the synthesis and use of cobalt-bearing cofactors (cobalamins) in their genomes. We explore cobalt metabolism in a *Prochlorococcus* isolate from the equatorial Pacific Ocean (strain MIT9215) through a series of growth experiments under iron- and cobalt-limiting conditions. Metal uptake rates, quantitative proteomic measurements of cobalamin-dependent enzymes, and theoretical calculations all indicate that *Prochlorococcus* MIT9215 can sustain growth with less than 50 cobalt atoms per cell, ∼100-fold lower than minimum iron requirements for these cells (∼5,100 atoms per cell). Quantitative descriptions of *Prochlorococcus* cobalt limitation are used to interpret the cobalt distribution in the equatorial Pacific Ocean, where surface concentrations are among the lowest measured globally but *Prochlorococcus* biomass is high. A low minimum cobalt quota ensures that other nutrients, notably iron, will be exhausted before cobalt can be fully depleted, helping to explain the persistence of cobalt-dependent metabolism in marine cyanobacteria.

Prochlorococcus | vitamin B12 | iron | Pacific Ocean | nutrient limitation

Cobalt is the least abundant elemental nutrient in seawater, but this may not have always been the case. In the modern ocean, cobalt scarcity develops from the oxidation of soluble Co^{2+} to insoluble Co^{3+} by Mn-oxidizing bacteria (1, 2), leaving behind a small pool of cobalt bound to strong organic ligands. Mn- and Co-oxidizing reactions are inhibited at low O_2, leading to the buildup of cobalt observed in oxygen-depleted waters (3–6). Similar reasoning has suggested that much higher cobalt inventories were found prior to the oxygenation of the oceans ∼300 million years ago (7, 8). Greater access to cobalt in the ancient anoxic ocean may have encouraged cobalt use in metalloenzymes, which evolved early in Earth's history (9, 10).

Since the oxidation of the oceans, there has been evolutionary selection against cobalt use over time, consistent with its decreasing availability (7, 11, 12). Eukaryotic genomes use cobalt less frequently than those of bacteria and archaea, and all eukaryotic organisms lack the ability for the de novo synthesis of cobalamin (vitamin B_{12}) from cobalt ion (13–15). The adoption of cobalamin-independent isoforms of methionine synthase, ribonucleotide reductase, and other enzymes has liberated land plants from cobalt dependence altogether (14, 16). Despite its scarcity and the availability of substitutes, there are benefits to cobalt use, exemplified among marine phytoplankton. For instance, 100-fold faster catalysis by cobalamin-dependent methionine synthase, MetH, compared to cobalamin-independent methionine synthase, MetE, allows for economization of nitrogen and other limiting resources (15, 17). Furthermore, Co^{2+} ions can activate Zn-dependent metalloenzymes like carbonic anhydrase, improving growth under Zn scarcity (18–20).

In the surface ocean, light inhibits bacterial Mn oxidation (21), but cobalt uptake by phytoplankton leads to the lowest concentrations at any depth, which can fall below 10^{-11} mol L^{-1} (10 pM; refs. 3, 6, and 22). There is growing evidence that the addition of cobalt or cobalamin to surface waters can increase phytoplankton growth rates when added in conjunction with other nutrients like iron and nitrogen (23–26). Yet, it is difficult to extrapolate these observations, because the cobalt requirements of some key phytoplankton taxa have not been quantified.

Emerging prior to the oxygenation of the oceans, marine cyanobacteria in the *Prochlorococcus* and *Synechococcus* lineage differ from eukaryotic phytoplankton in that they possess an absolute requirement for cobalt, independent of other nutrients like Zn (7, 18, 27, 28). Despite their minimal genomes, which contain nearly half as many genes as other cyanobacterial species (e.g., *Synechocystis*), all sequenced *Prochlorococcus* genomes have retained pathways for the de novo biosynthesis of pseudocobalamin (psB_{12}), a structural analog of vitamin B_{12} (29–31). The dominant phytoplankton group in the subtropical and tropical oceans, *Prochlorococcus* contributes a significant fraction of global

Significance

Photosynthetic phytoplankton are the foundation of marine ecosystems. Their growth in the sunlit ocean depends on ample supply of over a dozen essential elements. Of these elemental nutrients, the metal cobalt is found at the lowest concentrations in seawater, but it is unknown whether cobalt scarcity impacts phytoplankton growth. We have measured minimum cobalt requirements of the photosynthetic bacterium *Prochlorococcus*, which flourishes in nutrient-poor regions of the ocean where many other phytoplankton cannot survive. *Prochlorococcus* can grow with less than 50 cobalt atoms per cell, an extraordinarily small requirement that explains how this organism can persist in low-cobalt environments. These results enable predictions of how marine ecosystems respond to climate-driven changes in nutrient supply.

Author contributions: N.J.H., M.M.M., R.M.B., A.T., G.R.D., and M.A.S. designed research; N.J.H., M.M.M., R.M.B., A.T., T.J.G., D.M.M., L.V.-A., G.R.D., and M.A.S. performed research; N.J.H., M.M.M., R.M.B., A.T., T.J.G., D.M.M., L.V.-A., G.R.D., and M.A.S. analyzed data; and N.J.H. and M.A.S. wrote the paper with contributions from all authors.

The authors declare no competing interest.

This article is a PNAS Direct Submission.

Data deposition: Oceanographic data are deposited in Biological & Chemical Oceanography Data Management Office (BCO-DMO: https://www.bco-dmo.org/dataset/647250). Model output can be accessed at Zenodo, https://doi.org/10.5281/zenodo.3880520.

[1]Present address: Department of Oceanography, University of Hawaii at Manoa, Honolulu, HI 96822.

[2]To whom correspondence may be addressed. Email: hawco@hawaii.edu or msaito@whoi.edu.

This article contains supporting information online at https://www.pnas.org/lookup/suppl/doi:10.1073/pnas.2001393117/-/DCSupplemental.

primary production (32, 33), but the amount of cobalt needed to support this productivity is unknown. Here, we show that *Prochlorococcus* cells can grow with a very small number of cobalt atoms, enabling this organism to thrive in cobalt-poor environments like the equatorial Pacific Ocean without replacing cobalt-dependent metabolism.

Results and Discussion

Low Cobalt and Iron Requirements of *Prochlorococcus* MIT9215. To quantify cellular cobalt requirements, we conducted growth experiments in chemically defined media with axenic cultures of *Prochlorococcus* strain MIT9215, a member of the abundant high-light II clade that was originally isolated from the equatorial Pacific Ocean (34). While scarce iron in this region limits the growth of *Prochlorococcus* and other phytoplankton (35, 36), the tropical Pacific Ocean also hosts low cobalt concentrations [<10 pM (3, 23, 37)].

The influence of nutrient limitation on fitness is a function of two distinct traits: 1) the ability of a cell to acquire nutrients from seawater and 2) the ability to apply acquired nutrients toward the biosynthesis of compounds needed for growth and cell division (38). In our experiments, division rates of *Prochlorococcus* MIT9215 decreased when inorganic cobalt concentrations (Co′; see *Methods*) fell below 3 pM, and no growth was observed at a Co′ concentration below 0.1 pM (Fig. 1*A*). However, thresholds of Co′ in these experiments were highly sensitive to the concentrations of Zn and Mn present in the growth medium, due to competitive inhibition at the uptake site, and are difficult to relate to typical oceanic concentrations directly (39). Regardless, we observed a robust relationship between intracellular cobalt contents (the cobalt quota, Q_{Co}) and cell growth rate (μ; Fig. 1*B* and *SI Appendix*, Fig. S1). Growth of *Prochlorococcus* MIT9215 was well described by the Droop Equation,

$$\mu = \mu_{max}\left(1 - \frac{q_{min}}{Q_{Co}}\right), \quad [1]$$

which derives an absolute minimum quota, q_{min}, as growth rate (μ) approaches 0 (38). Least-squares fitting of q_{min} yielded extraordinarily low values: 14.8 ± 1.3 atoms per cell (R^2 = 0.96; equivalent to a cellular concentration of 220 nM). Implicit in this model is the expectation that increasing growth rates must be fueled by higher cobalt quotas, which is supported by our observations (Fig. 1*B*). From Eq. **1**, a growth-limited range (μ < 95% μ_{max}; *SI Appendix*, Table S1) can be identified when the cellular cobalt quota is ~300 atoms per cell or less, equal to a Co:Carbon ratio of $1.2 \pm 0.1 \times 10^{-7}$ (atom:atom). This value is similar to the Co:C ratio of a coastal *Synechococcus* under cobalt limitation [0.8×10^{-7} (18)], but an order of magnitude lower than the composite Co:C of eukaryotic phytoplankton [1.5×10^{-6} (40)], which is biochemically distinct from the cyanobacterial requirement and reflects variable substitution with Zn (18).

Cellular cobalt demands were compared to those of iron, the nutrient that limits *Prochlorococcus* growth in the equatorial Pacific Ocean (36). Growth limitation occurred when inorganic iron concentrations (Fe′) fell below 30 pM (Fig. 1*A*), similar to dissolved iron concentrations in the equatorial Pacific (41). To avoid iron limitation, *Prochlorococcus* MIT9215 required upward of 31,000 ± 3,400 Fe atoms per cell (μ < 95% μ_{max}, R^2 = 0.96; *SI Appendix*, Table S1), and estimated Fe:C ratios of iron-limited cells ($1.6 \pm 0.2 \times 10^{-5}$) were similar to Fe:C ratios of bulk particulate digestions from the equatorial Pacific, the closest approximation of *Prochlorococcus* metal quotas in situ (42). Iron requirements in *Prochlorococcus* MIT9215 were much lower than those reported for *Prochlorococcus* strain MED4 (Fe:C > 4.1×10^{-5}), which was isolated from the iron-rich Mediterranean Sea (43, 44), suggesting evolutionary pressure within this group to adapt to iron-poor regions of the oceans. The low Fe quotas of *Prochlorococcus* MIT9215 are still 100-fold larger than minimum cobalt requirements measured here (Fig. 1*B* and *SI Appendix*, Table S1).

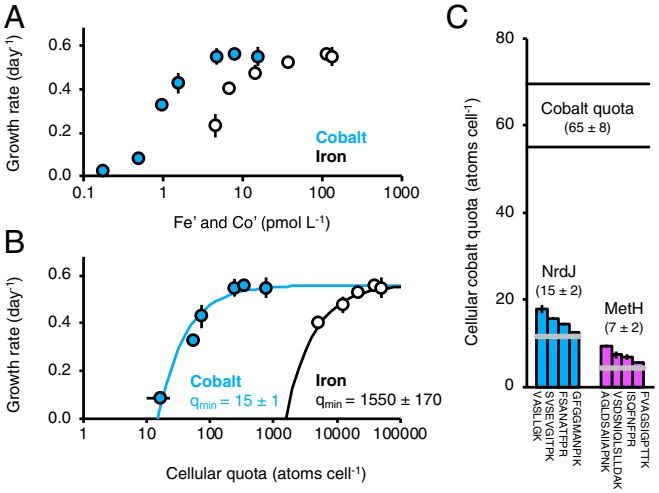

Fig. 1. Growth experiments with *Prochlorococcus* MIT9215, originally isolated from the equatorial Pacific Ocean. (*A*) The exponential growth rate of *Prochlorococcus* MIT9215 as a function of iron (white) and cobalt (blue) concentrations (calculated as the sum of inorganic metal species, Fe′ and Co′, in equilibrium with ethylenediaminetetraacetic acid [EDTA]; see *Methods*). (*B*) Dependence of specific growth rate on acquired Fe and Co (i.e., the cell quota), measured by ICP-MS. Lines show best fit curves for Eq. **1** and derived values of the minimum cell quota, q_{min} (R^2 = 0.96 for both elements). (*C*) Cell quotas (±1 SD) of cobalt, the cobalamin-dependent ribonucleotide reductase (NrdJ, blue), and the cobalamin-dependent methionine synthase (MetH, pink). Proteins were quantified by selected reaction monitoring of four tryptic peptides (colored bars) in large volume cultures of cobalt-limited *Prochlorococcus* MIT9215 (μ = 0.20 d^{-1}; *SI Appendix*, Table S7). Gray lines show predicted levels of these enzymes needed to support maximum growth rates (0.6 d^{-1}) observed in these experiments via use efficiency calculations (*SI Appendix*, Table S4).

Cobalt Use Efficiency in *Prochlorococcus*. Raven (45) originally defined a "metal use efficiency" by scaling in vitro enzyme rates with protein:metal stoichiometries to derive maximum rates of biomass production per atom of catalytic metal (45, 46). For example, given light-saturated rates of O_2 evolution at photosystem II and a stoichiometry of 20 iron atoms per photosynthetic unit (*SI Appendix*, Table S3), a photoautotrophic cell could be expected to grow at a rate of 1 mol C s^{-1}, per mol Fe (46). At this iron use efficiency, a cell the size of *Prochlorococcus* growing at a rate of 0.4 d^{-1} would need ~8,200 iron atoms per cell, similar to measured iron quotas at this growth rate (5,100 ± 1,100 atoms per cell; *SI Appendix*, Table S2). This is consistent with photosynthetic and respiratory enzymes being the dominant use for acquired iron in *Prochlorococcus*.

We sought to extend this metal use efficiency framework to cobalt. All sequenced *Prochlorococcus* genomes encode two cobalamin-dependent enzymes: 1) the ribonucleotide triphosphate reductase NrdJ, which generates deoxyribonucleotide bases (dNTPs) for DNA replication from ribonucleotide precursors, and 2) the methionine synthase MetH, which methylates homocysteine to generate the amino acid methionine, needed for protein synthesis (30, 47). Unlike plants and many eukaryotic phytoplankton (15), *Prochlorococcus* lacks cobalamin-independent versions of ribonucleotide reductase and methionine synthase, indicating that there is no substitute for cobalt requirements associated with NrdJ and MetH. Other characterized cobalamin- or Co^{2+}-dependent

enzymes, such as methylmalonyl CoA mutase and nitrile hydratase, are not present in the genome of *Prochlorococcus* MIT9215 or other sequenced *Prochlorococcus* strains.

Prior to dividing, *Prochlorococcus* MIT9215 must replicate its genome of 1.7 million base pairs, requiring dNTP synthesis via NrdJ. To grow at a rate of 0.6 d^{-1}, the maximum observed in our experiments and similar to in situ growth rates in the equatorial Pacific (36), at least 2.04 million dNTP bases per cell must be synthesized daily. In vitro characterizations of NrdJ show a maximum turnover time of two cycles per second: unimpeded, a single enzyme can produce 170,000 dNTP bases per day (48, 49). Assuming that the *Prochlorococcus* NrdJ can achieve similar rates in vivo, cellular demand for dNTPs would require at least 12 functioning copies of this enzyme to support maximum growth rates (*SI Appendix*, Table S4).

A much faster enzyme, MetH, can operate at over 18 cycles per second (17, 50). A single MetH enzyme can produce over 1.5 million methionine molecules per day. While a complex methionine cycle makes it challenging to predict cellular MetH demands (51), the cellular sulfur quota of roughly 12 million atoms (composed of methionine, cysteine and homocysteine thiols, sulfates, and sulfones, etc.) can serve as an upper bound (*SI Appendix*, Table S4). By this calculation, five copies of MetH would fulfill even this overestimated demand.

Given a 1:1 protein:cobalt stoichiometry evident from crystal structures of NrdJ and MetH, this analysis can account for 17 Co atoms in cobalamin-dependent enzymes for *Prochlorococcus* growing maximally, equivalent to a metal use efficiency of 6.6×10^7 mol C d^{-1} per mol Co. This estimate is fourfold higher than an empirical Co use efficiency of 1.6×10^7 calculated from growth experiments (*SI Appendix*, Tables S1 and S4), which may indicate the presence of additional Co associated with unknown enzymes, chaperones, and other transient reservoirs within the cell. To a first order, however, these calculations suggest that the quotas measured in *Prochlorococcus* cells are biochemically reasonable.

Mass Balance of Cobalt Metabolism. To validate the above calculations, we constructed ^{15}N-labeled peptide standards to quantify intracellular NrdJ and MetH levels by selected reaction monitoring mass spectrometry. From large volume cultures of cobalt-limited *Prochlorococcus* MIT9215 (μ = 0.2 d^{-1}), measurements of four tryptic peptides indicated that there were 15 ± 2 copies of NrdJ per cell (Fig. 1*C* and *SI Appendix*, Tables S5–S7). In the same sample, MetH was measured to an abundance of 7 ± 2 copies per cell. These measurements are remarkably consistent with predictions of 5 MetH and 12 NrdJ copies per cell based on the above use efficiency calculations at peak growth rates.

Still, the maximum amount of cobalt that can be attributed to use in NrdJ and MetH enzymes (22 ± 3 atoms per cell, assuming a 1:1 stoichiometry between Co and enzyme) is significantly less than the total cobalt quota in these cells, as measured by inductively coupled plasma mass spectrometry (ICP-MS; 62 ± 7 atoms per cell; Fig. 1*C*). Other reservoirs may account for more cobalt than NrdJ and MetH, even at these low intracellular concentrations. Before being used in NrdJ and MetH, acquired Co^{2+} ions must be transformed into pseudocobalamin (psB_{12}) cofactors, whose biosynthesis requires over a dozen enzymatic steps, beginning with the insertion of Co^{2+} into the corrinoid ring by the cobaltochelatase CbiK (14, 52). Given that many of the psB_{12} biosynthetic intermediates would be present at a steady-state concentration of a few copies per cell or less, the random walks of single molecules from the active site of one enzyme in the biosynthetic sequence to the next may be the rate-limiting step to *Prochlorococcus* growth under cobalt limitation. The sheer number of enzymatic alterations required to produce pseudocobalamin [>15 cobalt-bearing intermediates (12, 46)] probably acts as a limit to growth efficiency at low cobalt.

Perhaps related to these physical limits, there appears to be a lack of regulatory control on *Prochlorococcus* MIT9215 cobalt metabolism, at least by inorganic Co species. The abundance of NrdJ and MetH did not increase significantly at higher Co′, despite a 14-fold increase in cellular Co (54 to 780 atoms per cell; *SI Appendix*, Fig. S2*A*). Cobalt use efficiency calculations imply that the measured cellular inventory of NrdJ and MetH in cobalt-limited cells is sufficient to sustain the flux of dNTP and methionine needed to support maximum growth rates. When cellular cobalt quotas are growth limiting, it is likely that these enzymes are unsaturated with respect to their pseudocobalamin cofactors, decreasing their metabolic production and delaying cell division.

Furthermore, comparisons between the cellular proteomes of replete and cobalt-limited *Prochlorococcus* MIT9215 did not show large differences in protein abundance, with only 12% of detected proteins significantly different (*SI Appendix*, Fig. S2*B*). Stress-related proteins—the photosynthetic proteins PsaD, PsbO, and some ribosomal proteins—were somewhat higher in cobalt-limited cells, while adenosine 5′-triphosphate synthase and sugar metabolism genes were less abundant (*SI Appendix*, Table S8). As these proteins are associated with basic metabolic functions, it is likely that changes in the cell division rate, not cobalt itself, drive differences in the proteome under cobalt-limiting conditions. This is consistent with the absence of many cyanobacterial metal-sensing and regulatory genes in *Prochlorococcus* genomes (39, 53).

***Prochlorococcus* Co Nutrition in the Equatorial Pacific Ocean.** All sequenced *Prochlorococcus* isolates harbor genes for psB_{12} synthesis, as well as *nrdJ* and *metH*. It is expected that the cobalt requirements defined for the MIT9215 strain are broadly representative of all *Prochlorococcus* cells—at least as a lower limit—and can be used to investigate whether wild *Prochlorococcus* populations can meet their nutritional cobalt requirements.

To this end, we mapped the distribution of cobalt in the equatorial Pacific Ocean—the region where *Prochlorococcus* MIT9215 was originally isolated—from samples collected on the Metzyme expedition in October 2011 (Fig. 2*A*). Dissolved cobalt (dCo) was depleted in the surface ocean and accumulated in mesopelagic waters, consistent with the distribution of other phytoplankton nutrients like phosphate (Fig. 2 *B–D*). In the subsurface, cobalt concentrations greater than 100 pM were associated with very low oxygen waters (<50 μM; Fig. 2*E* and *SI Appendix*, Fig. S3*A*) that extend all of the way to the eastern margin (3). Sustained anoxia along the continental shelves of Peru and Mexico promotes the dissolution of cobalt bound in sedimentary Mn oxides (54, 55), and, at the basin scale, cobalt input from these reducing sediments is balanced by its removal onto Mn oxides formed in oxic waters (56). Inhibition of Mn and Co oxidation at low O_2, combined with significant regeneration of phytoplankton-derived cobalt, leads to plumes of high cobalt within low-oxygen waters in both the North and South Pacific (Fig. 2*C*).

At the equator, upwelling of subsurface waters from the Equatorial Undercurrent (EUC) leads to high nutrient concentrations and productivity. Originating in the oxygenated waters of the western Pacific, the EUC transports a large iron source from Papua New Guinea into the equatorial upwelling region (41, 57). As it travels eastward, the EUC splits low-oxygen water masses, leading to a downward deflection of O_2 contours between 2°N and 2°S (Fig. 2*B*) (58). Despite its importance as an iron source, cobalt concentrations within the EUC were not elevated (30 ± 2 pM between 100 and 250 m), especially compared to the surrounding low-oxygen waters (Fig. 2*C*). Low cobalt in the EUC probably reflects the high O_2 concentrations near Papua New Guinea and the predominance of oxic (rather than reducing) sedimentary sources (57, 59). Instead, entrainment of low-oxygen, high-cobalt waters into the EUC leads to elevated cobalt concentrations in the

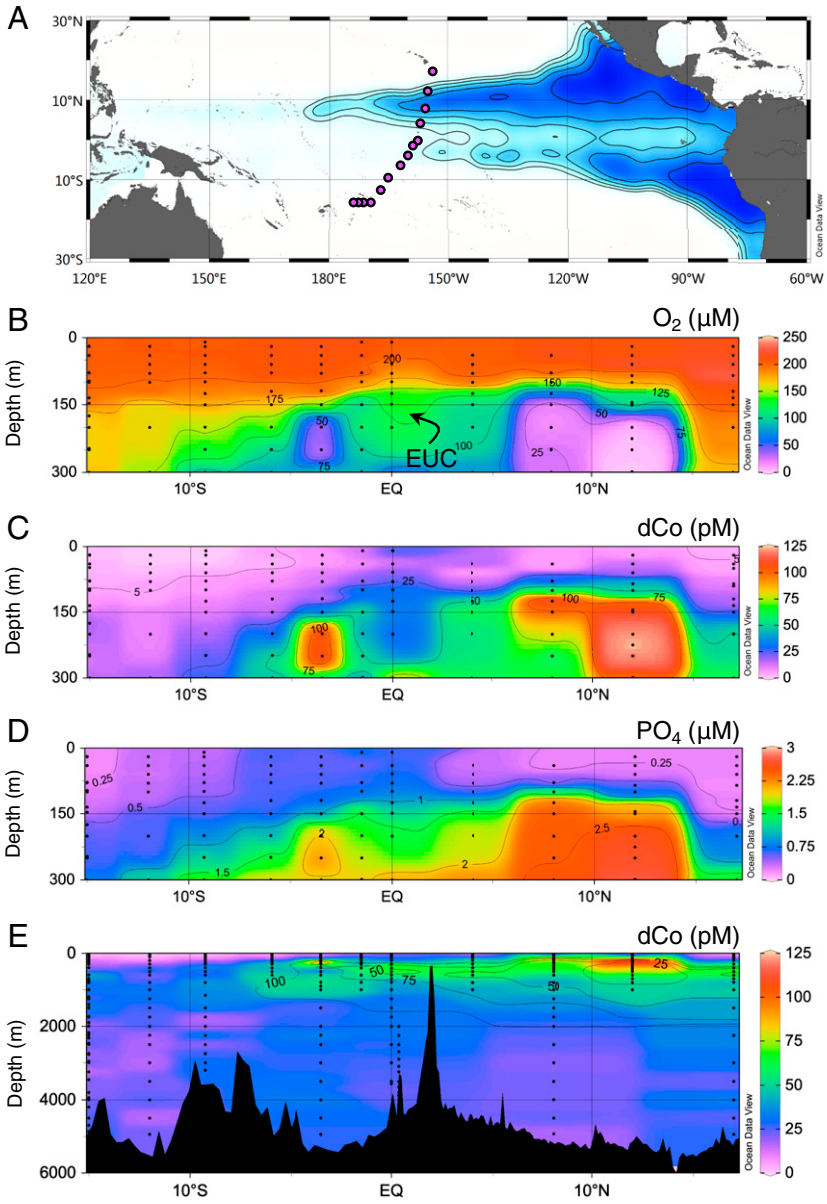

Fig. 2. The distribution of dissolved cobalt, dCo, in the equatorial Pacific Ocean. (*A*) Station locations (pink circles) from the Metzyme expedition (KM1128) relative to low-oxygen water masses originating on the Peruvian and Mexican margins. Contours mark 25-μM intervals in dissolved oxygen (O_2) between 25 μM and 100 μM at 200-m depth from the World Ocean Circulation Experiment (WOCE) gridded atlas (82). Blue shading highlights low dissolved oxygen. (*B*) A latitudinal section of dissolved oxygen concentrations from the Metzyme expedition. (*C*) dCo (operationally defined as the concentration passing through a 0.2-μm filter) and (*D*) dissolved phosphate (PO_4) along the same section. (*E*) The full depth distribution of dCo overlain with dissolved oxygen contours at 25-μM intervals between 0 and 100 μM O_2, which highlight their correlation throughout the water column (*SI Appendix*, Fig. S3).

euphotic zone at the equator (23 ± 6 pM between 0 and 100 m; Fig. 2*C*).

As upwelled equatorial waters are advected poleward, nutrient concentrations throughout the euphotic zone decrease due to uptake by phytoplankton. Interestingly, cobalt is more strongly depleted in the South Pacific Gyre than in the North Pacific, opposite to the trend in phosphate (compare, for instance, the 5-pM contour for cobalt in Fig. 2*B* and the 0.25-μM contour for PO_4 in Fig. 2*C*). Greater contact with coastal sources from East Asia, a larger oxygen minimum zone, and orders of magnitude greater deposition of desert dust in the Northern Hemisphere probably contribute to higher cobalt inventories in the North Pacific Subtropical Gyre (60–62). These sources are weaker in the South Pacific, allowing surface concentrations to fall below the 2-pM detection limit of our electrochemical method at both 9.2°S and 12°S (Fig. 3*A*). These stations also contained the largest populations of *Prochlorococcus* observed on the transect, evident in divinyl chlorophyll *a* concentrations [which are specific to *Prochlorococcus* (63)] that exceeded chlorophyll *a* produced by other phytoplankton (*SI Appendix*, Fig. S4). At a threshold growth rate of 95% μ_{max}, cobalt requirements of *Prochlorococcus* MIT9215 are estimated to be 300 atoms per cell, equivalent to a biomass Co:P ratio of 26×10^{-6} (*SI Appendix*, Table S1). Thus, in order to take up the 300 nM surface PO_4 found at 9.2°S and 12°S, *Prochlorococcus* must also acquire at least 7.8 pM Co in order to avoid cobalt-limited growth rates: more than triple the dCo concentration found at these stations. Indeed, dissolved Co:PO_4 ratios in the euphotic zone (0 to 100 m) fall below this threshold

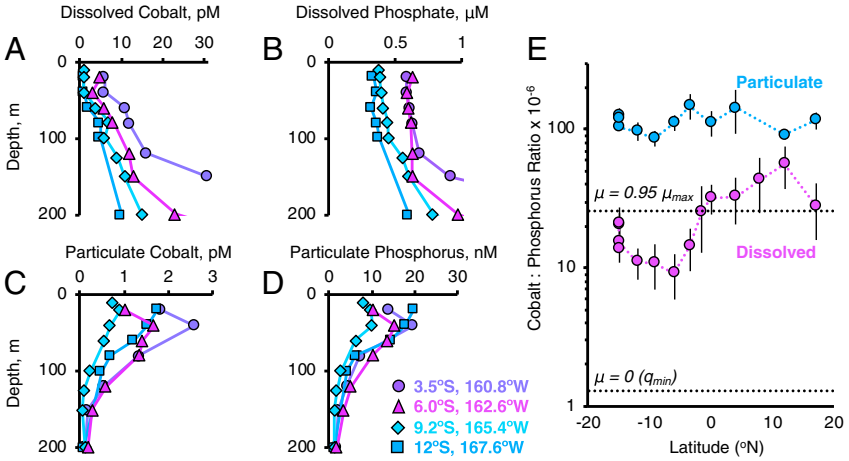

Fig. 3. Cobalt and phosphate profiles in the South Pacific Ocean from the Metzyme expedition. Removal of (*A*) dCo and (*B*) dissolved phosphate in the surface ocean is matched by surface maxima of (*C*) particulate cobalt and (*D*) particulate phosphorus. For *A*–*D*, colors and shapes indicate station locations. (*E*) The ratio of cobalt to phosphorus in the euphotic zone (0 to 100 m) along the Metzyme transect in both dissolved (pink) and particulate (blue) phases. Dotted black lines indicate the Co:P composition of cobalt-limited *Prochlorococcus* MIT9215 biomass at threshold growth rates of 0% and 95% μ_{max} via Eq. **1** (*SI Appendix*, Table S1).

for all stations south of the equator (Fig. 3*E*), suggesting that the PO_4 reservoir here cannot be depleted without forcing cobalt-limited growth rates.

However, elemental standing stocks do not always reflect their availability to organisms, many of which are adept at recycling trace nutrients. In the South Pacific, depletion of cobalt from the dissolved phase of seawater observed on the Metzyme expedition is mirrored by a significant accumulation of cobalt in particulate matter, often exceeding 1 pM (Fig. 3*C*). Correlation between pCo and particulate phosphorus indicates that pCo is primarily associated with biomass (Fig. 3*D* and *SI Appendix*, Fig. S3*B*). In both the North and South Pacific, the Co:P composition of particulate matter ($110 \pm 30 \times 10^{-6}$) exceeds both dissolved Co:PO_4 ratios and the cobalt limitation threshold of *Prochlorococcus* MIT9215 identified in culture (26×10^{-6}; Fig. 3*E*). To the extent that the Co:P composition of the total particulate pool reflects the composition of *Prochlorococcus* cells, it would appear that wild *Prochlorococcus* populations in the South Pacific have accumulated enough cobalt to satisfy their cobalamin metabolism and avoid cobalt limitation.

To understand how phytoplankton are able to accumulate Co in this region, we analyzed a global model of the marine cobalt cycle (37), which reproduces the very low dCo concentrations observed in the South Pacific but does not contain explicit parameterizations for Co limitation of phytoplankton growth. In the model, the South Pacific Gyre is the only region where dissolved Co:PO_4 ratios fall below the 95% μ_{max} threshold for *Prochlorococcus* MIT9215 [excluding the Southern Ocean where waters are too cold to support *Prochlorococcus* growth (64)]. Similar to our observations, the model also simulates elevated phytoplankton Co:P ratios in the South Pacific Gyre ($>100 \times 10^{-6}$), along with low dissolved Fe concentrations and Fe limitation of phytoplankton growth (*SI Appendix*, Figs. S5 and S6). Conceptually, iron-limited growth would allow the same number of cobalt transporters to complete more transport cycles prior to cell division, leading to a buildup of cellular Co. This effect is responsible for elevated phytoplankton Co:P ratios in the model, and was also observed during our iron limitation experiments with *Prochlorococcus* MIT9215 in culture (*SI Appendix*, Fig. S1 and Table S2). High levels of iron transporters and other protein biomarkers observed during the Metzyme expedition support model-based conclusions that iron limits *Prochlorococcus* growth in the South Pacific Gyre (*SI Appendix*, Fig. S7 and 35). Thus, cobalt accumulation afforded by iron-limited growth may be responsible for the high particulate Co:P ratios also observed on this transect.

Analysis of the measurements within the GEOTRACES intermediate data product (65) yields a similar conclusion: all waters with low Co:PO_4 ratios also contain comparatively lower Fe:PO_4 ratios (with respect to q_{min} values of Fe and Co determined from culture experiments; Fig. 4). If *Prochlorococcus* growth thresholds for cobalt and iron are assumed to be independent of one another (as in Liebig's law of the minimum), then cobalt limitation will be blocked by iron limitation (Fig. 4). Still, this scenario suggests that iron addition on short timescales (e.g., dust deposition) may drive *Prochlorococcus* and other phytoplankton toward cobalt limitation, consistent with observations of iron and cobalt colimitation in bottle incubations (23, 25).

There are two factors that complicate this interpretation. First, some *Prochlorococcus* lineages may retain a higher Co requirement than *Prochlorococcus* MIT9215, due to a reliance on other putative Co-dependent metalloenzymes, such as the PhoA alkaline phosphatase (30, 66). Second, in addition to *Prochlorococcus*, the pool of particulate matter in the surface ocean is also composed of small eukaryotic phytoplankton, mixotrophs, and grazers, as well as heterotrophic bacteria and detritus. Differences in cobalt (or P) accumulation between these reservoirs will distort comparisons with axenic *Prochlorococcus* cultures. Indeed, the cobalt requirements of eukaryotic phytoplankton like the diatom *Thalassiosira oceanica* and the haptophyte *Emiliana huxleyi* can be much greater than *Prochlorococcus* MIT9215 (Co:C $> 10^{-6}$ for both species) because these organisms substitute cobalt into their Zn-dependent enzymes (cambialism) when grown under low zinc concentrations found in open ocean environments (18, 19). Under conditions of Zn scarcity, the Co requirements of *E. huxleyi* can be more than 10-fold higher than *Prochlorococcus* MIT9215: equivalent to a biomass Co:P ratio greater than 300×10^{-6} (67). While the degree of Co–Zn interreplacement in the open ocean is currently unknown, dissolved Zn in the South Pacific Gyre can fall below 0.1 nM (65, 68), and free Zn′ concentrations are likely orders of magnitude lower due to complexation by organic ligands (69). When analyzing the Co:P ratio of a mixed assemblage, the potentially high Co:P ratios associated with cambialistic requirements may mask lower *Prochlorococcus* Co:P. Such high Co requirements must also make eukaryotic phytoplankton

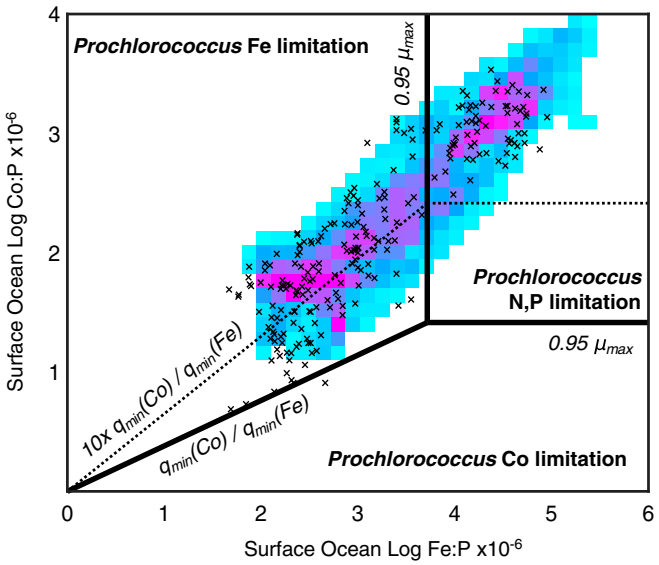

Fig. 4. Global analysis of cobalt depletion in the marine habitat of *Prochlorococcus,* defined as waters with temperature >12 °C. Colors represent the relative pixel density of modeled stoichiometry of total Co:PO_4 and Fe:PO_4 (the sum of dissolved and particulate phases) in the surface ocean, with pink colors indicating a large number of pixels (i.e., model grid cells). Crosses indicate measurements of dissolved Co, Fe, and PO_4 from the GEOTRACES Intermediate Data Product 2017 (65) from the surface mixed layer (0 to 30 m). Minimum Co and Fe requirements of *Prochlorococcus* MIT9215 are used to define growth limitation domains for Co and Fe (solid black lines). Dashed lines mark the shift in nutrient limitation domains if cobalt requirements increase by 10-fold (a Co:P ratio of 260×10^{-6} at 95% μ_{max}), which corresponds to Co:P ratios of *E. huxleyi* cultures grown in low-Zn media (67).

more susceptible to Co–Zn limitation. At the Co:P stoichiometry observed in *E. huxleyi*, the severity of Co depletion would exceed Fe throughout large areas of the North and South Pacific Oceans (Fig. 4 and *SI Appendix*, Fig. S8), possibly leading to Co–Zn limitation of growth. The simultaneous depletion of iron, nitrogen, cobalt, zinc, and other nutrients in the South Pacific and other subtropical gyres may prevent large-scale increases in ecosystem biomass, even if sources of the "limiting" nutrient are increased.

Evolutionary Drivers of Minimized Cobalt Metabolism. High cobalt concentrations in the equatorial Pacific are associated with oxygen-poor water masses, matching observations elsewhere in the Pacific and Atlantic (3, 6, 70). The worldwide association between Co and O_2 supports thermodynamic predictions that the anoxic ocean found during the Proterozoic and Archaean also contained much higher cobalt (7). As cyanobacteria evolved during this time, high cobalt availability probably facilitated the incorporation of (pseudo)cobalamin-dependent enzymes like NrdJ and MetH instead of other, cobalamin-independent versions of these proteins. However, genome-based timelines suggest that the *Prochlorococcus* lineage did not emerge until the late Paleoproterozoic or early Phanerozoic (28, 71). Although marine oxygen concentrations during this period are uncertain, the subsequent diversification of *Prochlorococcus* ecotypes throughout the Phanerozoic probably occurred in an oxygenated ocean (28, 72), with cobalt concentrations that were probably lower than when the cyanobacteria first evolved. As the evolution of *Prochlorococcus* ecotypes is characterized by metabolic streamlining and genome minimization (73, 74), it is interesting to note that, because all DNA bases in *Prochlorococcus* are synthesized by the NrdJ enzyme, decreasing genome size also helps to decrease cobalt requirements.

Our analysis suggests that *Prochlorococcus* cells can continue to function with a very small number of cobalt atoms, as low as 17 atoms per cell. While some lineages of *Prochlorococcus* may maintain a broader suite of cobalt-dependent or cambialistic enzymes (and therefore a higher cobalt requirement), the very low cobalt requirement of *Prochlorococcus* MIT9215 minimizes its exposure to cobalt-limiting conditions (Fig. 4), likely explaining the retention of psB_{12} biosynthesis in *Prochlorococcus* genomes. Similarity in proteomes between cobalt-replete and cobalt-limited growth suggests that *Prochlorococcus* MIT9215 does not actively monitor its cobalt inventory (*SI Appendix*, Fig. S2), nor does it make significant efforts to increase Co uptake by up-regulating Co′ transport systems. Indeed, Co′ uptake into *Prochlorococcus* MIT9215 cells appears to be relegated to the periplasmic Mn transport system MntABC, rather than a transporter specific to cobalt (39). These adaptations may reflect efforts to decrease the number of transporters and regulatory systems needed within the cell, a resource and energy savings that may offset the resource/energy expenditure associated with the production of psB_{12} biosynthetic enzymes.

While all sequenced *Prochlorococcus* genomes have retained the genes for psB_{12} biosynthesis, there are other cyanobacteria that have lost this functionality. For example, the benthic cyanobacterium *Synechococcus* PCC7002 has lost its cobalamin biosynthetic pathway and replaced its ancestral *nrdJ* with horizontally acquired *nrdAB* genes, which encode a B_{12}-independent ribonucleotide reductase (75, 76). As a result, *Synechococcus* PCC7002 depends on exogenous B_{12} to power the MetH methionine synthase. Genetic replacement of the *metH* gene with B_{12}-independent methionine synthase, *metE*, is sufficient to relieve *Synechococcus* PCC7002 of its B_{12} dependence (75). Several other cyanobacteria (e.g., *Synechococcus* PCC73109, *Crocosphaera watsonii*) have also acquired B_{12}-independent versions of both methionine synthase and ribonucleotide reductase. Given pervasive signals of horizontal gene acquisition in *Prochlorococcus* genomes (74), it is surprising that *metE* and *nrdAB* genes are absent from sequenced *Prochlorococcus* isolates.

Prochlorococcus appears to retain its psB_{12}-dependent enzymes out of physiological benefit rather than an insufficient access to B_{12}-independent alternatives. The cobalamin-independent ribonucleotide reductase NrdAB is an iron-dependent enzyme (77), whose incorporation would require an increase in *Prochlorococcus*'s iron requirement, making it less competitive in iron-limited waters. Similarly, B_{12}-independent MetE can only operate at ∼1% of the rate of MetH, and would therefore be needed at much higher quantity (15, 17), increasing demand for photosynthate (and therefore for Fe). Eukaryotic phytoplankton with both *metE* and *metH* genes clearly prefer to use MetH when B_{12} is present (15). The sheer abundance of *Prochlorococcus* throughout the subtropics and tropics implies that it is the major synthesizer of cobalamins throughout the sunlit ocean (29, 78, 79), and therefore supports the B_{12} dependencies of other phytoplankton [the pseudocobalamin produced by *Prochlorococcus* being convertible to conventional B_{12} by many species (29, 80)]. The persistence of psB_{12} biosynthesis in *Prochlorococcus* makes not only its own metabolism more efficient, but potentially the entire marine ecosystem.

Partially degraded B_{12} and psB_{12} molecules are inferred to be the major source of dCo ligands found in seawater, whose stability over hundreds of years protects cobalt in the ocean interior from scavenging by Mn-oxidizing bacteria and burial in marine sediments (23, 37, 56). Therefore, minimization—rather than replacement—of *Prochlorococcus* cobalamin-dependent metabolism may have a global effect on the marine cobalt cycle.

Methods

Axenic cultures of *Prochlorococcus* MIT9215 were grown, harvested, and analyzed as described previously (39). Growth rates were determined in

multiple 30-mL polycarbonate tubes and pooled to measure cellular metal quotas and protein content. Large (8 L) nonaxenic cultures were used to grow biomass for quantitative protein measurements.

Global and targeted protein measurements were made following previously described protocols (35, 81). Significantly different protein abundance was determined by the Fisher exact test using a cutoff of $P < 0.01$. Concentrations of *Prochlorococcus* MIT9215 ribonucleotide reductase (NrdJ) and methionine synthase (MetH) were measured in soluble protein extracts using ^{15}N-labeled peptide standards generated from *Prochlorococcus* NrdJ and MetH peptides in an *Escherichia coli* overexpression system. Labeled peptides were coexpressed with peptide sequences for horse myoglobin which were calibrated relative to a commercially available horse myoglobin protein (Fisher). Presence/absence of *nrdA, nrdJ, metE,* and *metH* was determined by Protein-Protein Basic Local Alignment Search Tool (BLASTp) searches with E-value cutoffs of 10^{-20}.

Concentrations of dCo (operationally defined as passing through a 0.2-μm filter) from the Metzyme expedition (KM1128) were measured by cathodic stripping voltammetry (3, 35). Sampling procedures and analysis of particulate metals is described by Saito et al. (35). Equations governing the Co biogeochemical model can be found elsewhere (37). Expanded methodological details can be found in *SI Appendix*.

Data Availability. Oceanographic data from the Metzyme expedition are accessible at the Biological and Chemical Oceanography Data Management Office repository (https://www.bco-dmo.org/project/2236). Data tables for culture experiments are provided in *SI Appendix*. Model output can be accessed at Zenodo, https://doi.org/10.5281/zenodo.3880520.

ACKNOWLEDGMENTS. We are grateful to the Captain and crew of the R/V *Kilo Moana* for their assistance on the KM1128 expedition and to co-chief scientist Carl Lamborg. We thank John Waterbury for allowing us access to incubators, as well as Alison Coe and the Chisholm laboratory at Massachusetts Institute of Technology for providing *Prochlorococcus* cultures. We also thank Elizabeth Kujawinski, Mick Follows, Phoebe Lam, and three anonymous reviewers for constructive feedback on this work. This work was supported by the Gordon and Betty Moore Foundation Grants 3782 and 3934 (to M.A.S.), and NSF Awards OCE-1031271, OCE-1658030, OCE-1850719, and OCE-1924554 (to M.A.S.). A.T. received funding from the European Research Council under the European Union's Horizon 2020 research and innovation program (Grant Agreement 724289). The writing of the manuscript was supported by a Simons Foundation Life Sciences Postdoctoral Fellowship to N.J.H. (Fellowship 602538).

1. J. W. Moffett, J. Ho, Oxidation of cobalt and manganese in seawater via a common microbially catalyzed pathway. *Geochim. Cosmochim. Acta* **60**, 3415–3424 (1996).
2. B. Lee, N. S. Fisher, Microbially mediated cobalt oxidation in seawater revealed by radiotracer experiments. *Limnol. Oceanogr.* **38**, 1593–1602 (1993).
3. N. J. Hawco, D. C. Ohnemus, J. A. Resing, B. S. Twining, M. A. Saito, A cobalt plume in the oxygen minimum zone of the Eastern Tropical South Pacific. *Biogeosciences* **13**, 5697–5717 (2016).
4. D. C. Ohnemus *et al.*, Elevated trace metal content of prokaryotic plankton communities associated with marine oxygen deficient zones. *Limnol. Oceanogr.* **62**, 3–25 (2017).
5. K. S. Johnson, K. H. Coale, W. M. Berelson, R. Michael Gordon, On the formation of the manganese maximum in the oxygen minimum. *Geochim. Cosmochim. Acta* **60**, 1291–1299 (1996).
6. A. E. Noble *et al.*, Basin-scale inputs of cobalt, iron, and manganese from the Benguela-Angola front to the South Atlantic Ocean. *Limnol. Oceanogr.* **57**, 989–1010 (2012).
7. M. A. Saito, D. M. Sigman, F. M. Morel, The bioinorganic chemistry of the ancient ocean: The co-evolution of cyanobacterial metal requirements and biogeochemical cycles at the Archean–Proterozoic boundary? *Inorg. Chim. Acta* **356**, 308–318 (2003).
8. E. D. Swanner *et al.*, Cobalt and marine redox evolution. *Earth Planet. Sci. Lett.* **390**, 253–263 (2014).
9. M. C. Weiss *et al.*, The physiology and habitat of the last universal common ancestor. *Nat. Microbiol.* **1**, 16116 (2016).
10. D. Lundin, G. Berggren, D. T. Logan, B. M. Sjöberg, The origin and evolution of ribonucleotide reduction. *Life (Basel)* **5**, 604–636 (2015).
11. C. L. Dupont, A. Butcher, R. E. Valas, P. E. Bourne, G. Caetano-Anollés, History of biological metal utilization inferred through phylogenomic analysis of protein structures. *Proc. Natl. Acad. Sci. U.S.A.* **107**, 10567–10572 (2010).
12. J. J. R. F. da Silva, R. J. P. Williams, *The Biological Chemistry of the Elements: The Inorganic Chemistry of Life*, (Oxford University Press, Oxford, United Kingdom, 1991).
13. C. L. Dupont, S. Yang, B. Palenik, P. E. Bourne, Modern proteomes contain putative imprints of ancient shifts in trace metal geochemistry. *Proc. Natl. Acad. Sci. U.S.A.* **103**, 17822–17827 (2006).
14. D. A. Rodionov, A. G. Vitreschak, A. A. Mironov, M. S. Gelfand, Comparative genomics of the vitamin B12 metabolism and regulation in prokaryotes. *J. Biol. Chem.* **278**, 41148–41159 (2003).
15. E. M. Bertrand *et al.*, Methionine synthase interreplacement in diatom cultures and communities: Implications for the persistence of B_{12} use by eukaryotic phytoplankton. *Limnol. Oceanogr.* **58**, 1431–1450 (2013).
16. Y. Zhang, D. A. Rodionov, M. S. Gelfand, V. N. Gladyshev, Comparative genomic analyses of nickel, cobalt and vitamin B12 utilization. *BMC Genomics* **10**, 78 (2009).
17. R. V. Banerjee, V. Frasca, D. P. Ballou, R. G. Matthews, Participation of cob(I) alamin in the reaction catalyzed by methionine synthase from *Escherichia coli*: A steady-state and rapid reaction kinetic analysis. *Biochemistry* **29**, 11101–11109 (1990).
18. W. G. Sunda, S. A. Huntsman, Cobalt and zinc interreplacement in marine phytoplankton: Biological and geochemical implications. *Limnol. Oceanogr.* **40**, 1404–1417 (1995).
19. D. Yee, F. M. M. Morel, In vivo substitution of zinc by cobalt in carbonic anhydrase of a marine diatom. *Limnol. Oceanogr.* **41**, 573–577 (1996).
20. N. M. Price, F. M. M. Morel, Cadmium and cobalt substitution for zinc in a marine diatom. *Nature* **344**, 658–660 (1990).
21. W. G. Sunda, S. A. Huntsman, Effect of sunlight on redox cycles of manganese in the southwestern Sargasso Sea. *Deep-Sea Res. A, Oceanogr. Res. Pap.* **35**, 1297–1317 (1988).
22. A. E. Noble, M. A. Saito, K. Maiti, C. R. Benitez-Nelson, Cobalt, manganese, and iron near the Hawaiian Islands: A potential concentrating mechanism for cobalt within a cyclonic eddy and implications for the hybrid-type trace metals. *Deep Sea Res. Part II Top. Stud. Oceanogr.* **55**, 1473–1490 (2008).
23. M. A. Saito, G. Rocap, J. W. Moffett, Production of cobalt binding ligands in a *Synechococcus* feature at the Costa Rica upwelling dome. *Limnol. Oceanogr.* **50**, 279–290 (2005).
24. E. M. Bertrand *et al.*, Vitamin B_{12} and iron colimitation of phytoplankton growth in the Ross Sea. *Limnol. Oceanogr.* **52**, 1079–1093 (2007).
25. T. J. Browning *et al.*, Nutrient co-limitation at the boundary of an oceanic gyre. *Nature* **551**, 242–246 (2017).
26. J. H. Martin, R. M. Gordon, S. Fitzwater, W. W. Broenkow, Vertex: Phytoplankton/iron studies in the Gulf of Alaska. *Deep-Sea Res. A, Oceanogr. Res. Pap.* **36**, 649–680 (1989).
27. M. A. Saito, J. W. Moffett, S. W. Chisholm, J. B. Waterbury, Cobalt limitation and uptake in *Prochlorococcus*. *Limnol. Oceanogr.* **47**, 1629–1636 (2002).
28. P. Sánchez-Baracaldo, Origin of marine planktonic cyanobacteria. *Sci. Rep.* **5**, 17418 (2015).
29. K. R. Heal *et al.*, Two distinct pools of B_{12} analogs reveal community interdependencies in the ocean. *Proc. Natl. Acad. Sci. U.S.A.* **114**, 364–369 (2017).
30. S. J. Biller *et al.*, Genomes of diverse isolates of the marine cyanobacterium *Prochlorococcus*. *Sci. Data* **1**, 140034 (2014).
31. G. Rocap *et al.*, Genome divergence in two *Prochlorococcus* ecotypes reflects oceanic niche differentiation. *Nature* **424**, 1042–1047 (2003).
32. Y. M. Rii, D. M. Karl, M. J. Church, Temporal and vertical variability in picophytoplankton primary productivity in the North Pacific Subtropical Gyre. *Mar. Ecol. Prog. Ser.* **562**, 1–18 (2016).
33. H. Liu, H. A. Nolla, L. Campbell, *Prochlorococcus* growth rate and contribution to primary production in the equatorial and subtropical North Pacific Ocean. *Aquat. Microb. Ecol.* **12**, 39–47 (1997).
34. G. C. Kettler *et al.*, Patterns and implications of gene gain and loss in the evolution of *Prochlorococcus*. *PLoS Genet.* **3**, e231 (2007).
35. M. A. Saito *et al.*, Multiple nutrient stresses at intersecting Pacific Ocean biomes detected by protein biomarkers. *Science* **345**, 1173–1177 (2014).
36. E. L. Mann, S. W. Chisholm, Iron limits the cell division rate of *Prochlorococcus* in the eastern equatorial Pacific. *Limnol. Oceanogr.* **45**, 1067–1076 (2000).
37. A. Tagliabue *et al.*, The role of external inputs and Internal cycling in shaping the global ocean cobalt distribution: Insights from the first cobalt biogeochemical model. *Global Biogeochem. Cycles* **32**, 594–616 (2018).
38. M. R. Droop, Some thoughts on nutrient limitation in algae. *J. Phycol.* **9**, 264–272 (1973).
39. N. J. Hawco, M. A. Saito, Competitive inhibition of cobalt uptake by zinc and manganese in a Pacific *Prochlorococcus* strain: Insights into metal homeostasis in a streamlined oligotrophic cyanobacterium. *Limnol. Oceanogr.* **63**, 2229–2249 (2018).
40. T. Ho *et al.*, The elemental composition of some marine phytoplankton. *J. Phycol.* **39**, 1145–1159 (2003).
41. K. H. Coale, S. E. Fitzwater, R. M. Gordon, K. S. Johnson, R. T. Barber, Control of community growth and export production by upwelled iron in the equatorial Pacific Ocean. *Nature* **379**, 1994–1997 (1996).
42. B. S. Twining *et al.*, Metal quotas of plankton in the equatorial Pacific Ocean. *Deep Sea Res. Part II Top. Stud. Oceanogr.* **58**, 325–341 (2011).
43. B. R. Cunningham, S. G. John, The effect of iron limitation on cyanobacteria major nutrient and trace element stoichiometry. *Limnol. Oceanogr.* **62**, 846–858 (2017).
44. D. M. Shire, A. B. Kustka, Luxury uptake, iron storage and ferritin abundance in *Prochlorococcus marinus (Synechococcales)* strain MED4. *Phycologia* **54**, 398–406 (2015).
45. J. A. Raven, The iron and molybdenum use efficiencies of plant growth with different energy, carbon and nitrogen sources. *New Phytol.* **109**, 279–288 (1988).
46. J. A. Raven, Predictions of Mn and Fe use efficiencies of phototrophic growth as a function of light availability for growth and of C assimilation pathway. *New Phytol.* **116**, 1–18 (1990).
47. C. W. Goulding, D. Postigo, R. G. Matthews, Cobalamin-dependent methionine synthase is a modular protein with distinct regions for binding homocysteine, methyltetrahydrofolate, cobalamin, and adenosylmethionine. *Biochemistry* **36**, 8082–8091 (1997).

48. S. S. Licht, C. C. Lawrence, J. Stubbe, Class II ribonucleotide reductases catalyze carbon-cobalt bond reformation on every turnover. *J. Am. Chem. Soc.* **121**, 7463–7468 (1999).
49. S. Booker, S. Licht, J. Broderick, J. Stubbe, Coenzyme B12-dependent ribonucleotide reductase: Evidence for the participation of five cysteine residues in ribonucleotide reduction. *Biochemistry* **33**, 12676–12685 (1994).
50. C. W. Goulding, R. G. Matthews, Cobalamin-dependent methionine synthase from *Escherichia coli:* Involvement of zinc in homocysteine activation. *Biochemistry* **36**, 15749–15757 (1997).
51. M. Sauter, B. Moffatt, M. C. Saechao, R. Hell, M. Wirtz, Methionine salvage and S-adenosylmethionine: Essential links between sulfur, ethylene and polyamine biosynthesis. *Biochem. J.* **451**, 145–154 (2013).
52. S. J. Moore *et al*., Elucidation of the anaerobic pathway for the corrin component of cobalamin (vitamin B12). *Proc. Natl. Acad. Sci. U.S.A.* **110**, 14906–14911 (2013).
53. N. A. Held, M. R. McIlvin, D. M. Moran, M. T. Laub, M. A. Saito, Unique patterns and biogeochemical relevance of two-component sensing in marine bacteria. *mSystems* **4**, e00317-18 (2019).
54. K. S. Johnson, P. M. Stout, W. M. Berelson, C. M. Sakamoto-Arnold, Cobalt and copper distributions in the waters of Santa Monica Basin, California. *Nature* **332**, 527–530 (1988).
55. P. Böning *et al*., Geochemistry of Peruvian near-surface sediments. *Geochim. Cosmochim. Acta* **68**, 4429–4451 (2004).
56. N. J. Hawco *et al*., Cobalt scavenging in the mesopelagic ocean and its influence on global mass balance : Synthesizing water column and sedimentary fluxes. *Mar. Chem.* **201**, 151–166 (2018).
57. L. O. Slemons, J. W. Murray, J. Resing, B. Paul, P. Dutrieux, Western Pacific coastal sources of iron, manganese, and aluminum to the Equatorial Undercurrent. *Global Biogeochem. Cycles* **24**, GB3024 (2010).
58. L. Stramma, G. C. Johnson, E. Firing, S. Schmidtko, Eastern Pacific oxygen minimum zones: Supply paths and multidecadal changes. *J. Geophys. Res.* **115**, C09011 (2010).
59. A. Radic, F. Lacan, J. W. Murray, Iron isotopes in the seawater of the equatorial Pacific Ocean: New constraints for the oceanic iron cycle. *Earth Planet. Sci. Lett.* **306**, 1–10 (2011).
60. N. M. Mahowald *et al*., Atmospheric global dust cycle and iron inputs to the ocean. *Global Biogeochem. Cycles* **19**, GB4025 (2005).
61. E. Y. Kwon *et al*., Global estimate of submarine groundwater discharge based on an observationally constrained radium isotope model. *Geophys. Res. Lett.* **41**, 8438–8444 (2014).
62. J. Karstensen, L. Stramma, M. Visbeck, Oxygen minimum zones in the eastern tropical Atlantic and Pacific oceans. *Prog. Oceanogr.* **77**, 331–350 (2008).
63. G. R. Ditullio *et al*., Phytoplankton assemblage structure and primary productivity along 170° W in the South Pacific Ocean. *Mar. Ecol. Prog. Ser.* **255**, 55–80 (2003).
64. E. R. Zinser *et al*., Influence of light and temperature on *Prochlorococcus* ecotype distributions in the Atlantic Ocean. *Limnol. Oceanogr.* **52**, 2205–2220 (2007).
65. R. Schlitzer *et al*., The GEOTRACES Intermediate Data Product 2017. *Chem. Geol.* **493**, 210–223 (2018).
66. M. A. Saito *et al*., The acceleration of dissolved cobalt's ecological stoichiometry due to biological uptake, remineralization, and scavenging in the Atlantic Ocean. *Biogeosciences* **14**, 4637–4662 (2017).
67. Y. Xu, D. Tang, Y. Shaked, F. M. M. Morel, Zinc, cadmium, and cobalt interreplacement and relative use efficiencies in the coccolithophore *Emiliania huxleyi*. *Limnol. Oceanogr.* **52**, 2294–2305 (2007).
68. S. G. John, J. Helgoe, E. Townsend, Biogeochemical cycling of Zn and Cd and their stable isotopes in the Eastern Tropical South Pacific. *Mar. Chem.* **201**, 256–262 (2018).
69. K. W. Bruland, Complexation of zinc by natural organic ligands in the central North Pacific. *Limnol. Oceanogr.* **34**, 269–285 (1989).
70. A. E. Noble, D. C. Ohnemus, N. J. Hawco, P. J. Lam, M. A. Saito, Coastal sources, sinks and strong organic complexation of dissolved cobalt within the US North Atlantic GEOTRACES transect GA03. *Biogeosciences* **14**, 2715–2739 (2017).
71. R. Braakman, M. J. Follows, S. W. Chisholm, Metabolic evolution and the self-organization of ecosystems. *Proc. Natl. Acad. Sci. U.S.A.* **114**, E3091–E3100 (2017).
72. E. A. Sperling *et al*., Statistical analysis of iron geochemical data suggests limited late Proterozoic oxygenation. *Nature* **523**, 451–454 (2015).
73. F. Partensky, L. Garczarek, *Prochlorococcus*: Advantages and limits of minimalism. *Annu. Rev. Mar. Sci.* **2**, 305–331 (2010).
74. S. J. Biller, P. M. Berube, D. Lindell, S. W. Chisholm, *Prochlorococcus*: The structure and function of collective diversity. *Nat. Rev. Microbiol.* **13**, 13–27 (2015).
75. A. A. Pérez, Z. Liu, D. A. Rodionov, Z. Li, D. A. Bryant, Complementation of cobalamin Auxotrophy in *Synechococcus sp.* strain PCC 7002 and validation of a putative cobalamin riboswitch in vivo. *J. Bacteriol.* **198**, 2743–2752 (2016).
76. S. W. Wilhelm, C. G. Trick, Effects of vitamin B12 concentration on chemostat cultured *Synechococcus Sp* strain PCC 7002. *Can. J. Microbiol.* **41**, 145–151 (1995).
77. M. Kolberg, K. R. Strand, P. Graff, K. K. Andersson, Structure, function, and mechanism of ribonucleotide reductases. *Biochim. Biophys. Acta* **1699**, 1–34 (2004).
78. A. C. Doxey, D. A. Kurtz, M. D. J. Lynch, L. A. Sauder, J. D. Neufeld, Aquatic metagenomes implicate *Thaumarchaeota* in global cobalamin production. *ISME J.* **9**, 461–471 (2015).
79. P. Flombaum *et al*., Present and future global distributions of the marine Cyanobacteria *Prochlorococcus* and *Synechococcus*. *Proc. Natl. Acad. Sci. U.S.A.* **110**, 9824–9829 (2013).
80. K. E. Helliwell *et al*., Cyanobacteria and eukaryotic algae use different chemical variants of vitamin B12. *Curr. Biol.* **26**, 999–1008 (2016).
81. M. A. Saito *et al*., Iron conservation by reduction of metalloenzyme inventories in the marine diazotroph *Crocosphaera watsonii*. *Proc. Natl. Acad. Sci. U.S.A.* **108**, 2184–2189 (2011).
82. V. Gouretski, K. P. Koltermann, WOCE global hydrographic climatology. *Berichte des BSH* **35**, 1–52 (2004).